Journal of Porphyrins and Phthalocyanines
J. Porphyrins Phthalocyanines 2001; **5**: 58–66

Triplet porphyrins as donors in intramolecular electron transfer and their intermolecular interaction with free radicals

A. BLANK, T. GALILI and H. LEVANON*

Department of Physical Chemistry and the Farkas Center for Light-Induced Processes, The Hebrew University of Jerusalem, 91904 Jerusalem, Israel

Received 7 January 2000
Accepted 21 February 2000

ABSTRACT: Porphyrins and related compounds are basic moieties which upon photoexcitation produce paramagnetic transients important to many processes in biology, material science and light–energy conversion. This short review demonstrates the application of time-resolved EPR spectroscopy to two processes in which the photoexcited singlet and/or triplet are involved: (1) intramolecular electron transfer in photoexcited donor–acceptor systems embedded in liquid crystals, where the porphyrins are the electron donors attached to different types of acceptors; and (2) intermolecular magnetic interactions between photoexcited porphyrin triplets and free radicals. In both systems the electron spin plays an important part with regards to the route of the magnetic interactions involved.

KEYWORDS: EPR; spin polarization; electron transfer; CIDEP; RTPM; ESPT

INTRODUCTION

Photophysical and photochemical processes in which optical excitation results in molecular change through optically excited states are of considerable importance. In terms of natural phenomena, photosynthesis is the most known and widespread process which involves many photophysical aspects [1]. In terms of man-made applications, one can mention photoinduced electron transfer (ET) which may be used in molecular-sized switches [2] or photorefractive materials [3]. In a different area, one may exploit the phenomenon of chemically induced spin polarization (CIDEP) for several electromagnetic applications [4]. In a substantial number of these photophysical processes the electron spin plays an important role in the reaction and its evolution either through a single- or a multi-step reaction. The unpaired electron can be monitored efficiently in most of these cases by time-resolved EPR (TREPR).

The chemical entities, i.e. the porphyrins, which absorb visible light in the singlet manifold and transform into the triplet state are considered as most important compounds with respect to their photophysical properties. Our studies with these compounds have concentrated on two main photophysical processes, namely intramolecular electron transfer (IET), which is depicted in Fig. 1, and intermolecular radical–photoinduced triplet interaction. These interactions exemplify the important role of the electron spin in these processes and also the usefulness of TREPR spectroscopy in exploring these reactions. In addition, the solvent properties play a crucial role in these types of reactions, in particular liquid crystals (LCs) with their unique dielectric properties.

In the first part we shall show how the dielectric properties of LCs are exploited to obtain wide temperature-dependent TREPR spectra which shed light on the mechanism and spin dynamics of IET processes. We shall also demonstrate how the absolute values of the radical pair (RP) energy states can be determined. The second part, which is related to the photophysics of porphyrins, shows how the magnetic interaction between the prophyrin's photoexcited triplet state and a stable paramagnetic radical, in thermal spin distribution, induces a unique non-Boltzmann distribution in the stable radical. This spin polarization is attributed to the interaction between the quartet and doublet states during the encounter between the photoexcited triplet and the stable radical. As of today, we have found that these magnetic interactions are stronger in porphyrins than in any other triplet we have examined.

EXPERIMENTAL

Intramolecular Electron Transfer (IET) Experiments

Covalently linked donor–spacer–acceptor (D–*s*–A) systems were synthesized by Wasielewski and co-workers [5] (zinc 9-desoxomethylpyropheophorbide *a*, pyromellitimide, 1, 8:4,5-naphtalenediimide and their compounds) and Kurreck

---

*Correspondence to: H. Levanon, Department of Physical Chemistry and the Farkas Center for Light-Induced Processes, The Hebrew University of Jerusalem, 91904 Jerusalem, Israel.

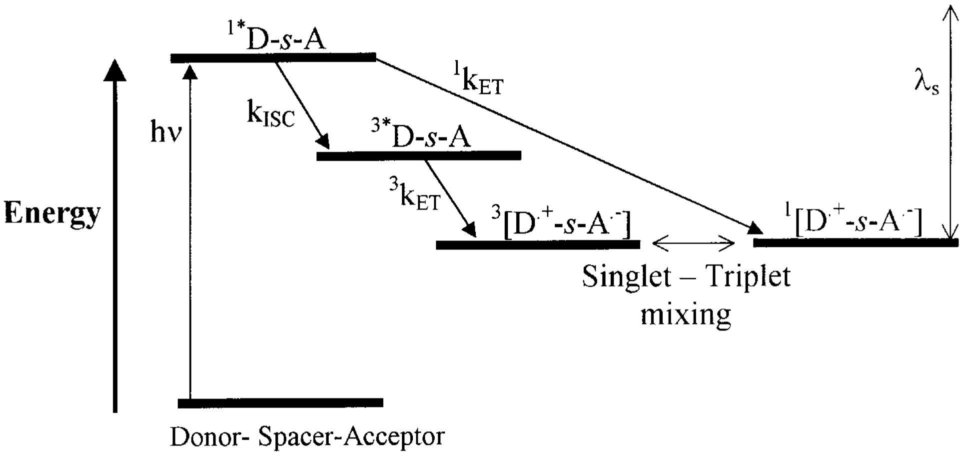

Fig. 1. Energy levels of a donor–spacer–acceptor (D–*s*–A) supramolecular system under photoexcitation. D is photoexcited by a laser pulse at a selective wavelength. This event starts the series of ET reactions, producing the different paramagnetic transients. λ_s represents the temperature-dependent reorganization energy.

and co-workers [6], while base-paired porphyrin–quinone systems were synthesized by Sessler *et al.* [7, 8].

TREPR experiments were performed by measuring the time-dependent EPR signal after selective wavelength laser excitation (Continuum model 661-2D laser). The signal generated under CW microwave irradiation (Bruker ESP 380E) was taken from the preamplifier, which is connected directly to the microwave diode detector, and was fed into a digitizer interfaced to a computer that monitored the experiment [9]. A series of complete TREPR spectra, at different delay times after the laser pulse, was reconstructed from the EPR kinetic traces of $M_y(t)$ by slowly stepping up the magnetic field. Samples were prepared by dissolving the compounds in LCs in 4 mm o.d. and 2.8 mm i.d. Pyrex tubes, degassed by several freeze–pump–thaw cycles on a vacuum line. The temperature was maintained using a nitrogen variable-temperature flow dewar in the EPR resonator. The samples in LCs were aligned in the magnetic field by heating them to temperatures above the clearing point of the LC in a high magnetic field; followed by cooling to the freezing temperature [10]. Typical spectra were taken at two sample orientations in terms of the LC director **L** with respect to the external magnetic field **B**, i.e. $\mathbf{L} \parallel \mathbf{B}$ and $\mathbf{L} \perp \mathbf{B}$.

Triplet–Radical Interaction Experiments

H_2TPP (tetraphenylporphyrin), the stable radicals galvinoxyl and BDPA (2,6-di-*tert*-butyl-*a*-(3,5-di-*tert*-butyl-4-oxo-2,5-cyclohexadien-1-ylidene)-*p*-tolyloxy and bisdiphenylene-β-phenylallyl respectively), toluene (Aldrich), ZnTPP (zinc tetraphenylporphyrin) (Midcentury Chemical Company), dichloromethane and heavy paraffin oil (Sigma) were used. Samples in toluene were prepared by dissolving both galvinoxyl (gal) and the porphyrin, while samples in paraffin oil were prepared by first dissolving BDPA and the porphyrin in dichloromethane and then diluting them in paraffin oil (20% dichloromethane and 80% paraffin). The solutions were poured into Pyrex EPR tubes and sealed under vacuum after several freeze–thaw cycles. FT-EPR measurements were performed with a Bruker ESP 380E spectrometer. The porphyrins in the mixtures were photoexcited by a pulsed laser as described above ($\lambda = 532$ nm, pulse duration 12 ns, pulse repetition rate 20 Hz, pulse energy 5 mJ per pulse). The chromophore concentration was ~5 mM and the radical concentration was ~2 mM in all samples.

INTRAMOLECULAR ELECTRON TRANSFER

General Background

The understanding of light-induced ET processes in photosynthesis and model systems has advanced significantly during recent years [11]. The complexity of natural photosynthetic systems has prompted studies of simpler model systems that might reproduce essential features of the biological target. Most current model ET studies use the porphyrin moiety as a leading structure. Although simple porphyrins in intermolecular ET fail to mimic natural photosynthesis, they are important in implementing the mechanistic strategy. On the other hand, the covalently linked porphyrins–quinones are becoming more useful in the mechanistic approach by providing mimics for singlet-initiated ET and long-lived charge-separated states [12, 13].

An important aspect of the model systems is the matrices in which they are embedded. LCs provide suitable anisotropic media for large and small chromophores such as porphyrins, chlorophylls [10, 14] and covalently linked ensembles of donor–spacer–acceptor (D–*s*–A), where D and A are porphyrins and quinones respectively [15]. Moreover, the range of TREPR detection of transient radical pairs (RPs) embedded in LCs can be spanned over a wide temperature range (about 120 K) including ambient temperatures. Most importantly, the IET rates in these solvents are reduced by several orders of magnitude (from picoseconds to nanoseconds), permitting the observation of these processes on submicrosecond timescales. The reduction of IET rates is due to the nematic potential associated with the alignment of the LC molecules, which restricts the isotropic molecular reorientation found in conventional solvents [15, 16].

Mechanistic Approach of Model Photosynthesis

One of the major goals in the mechanistic approach of model photosynthesis is to reproduce the electronic states associated with basic features of the IET process and charge separation. Thus a simplified model system consists of a D–*s*–A ensemble combined with the matrix in which the supramolecule is embedded. In most of our studies, LCs were found to be the most suitable matrices. The high time resolution of TREPR makes this spectroscopy suitable for characterizing ET reactions in different molecular systems. Of the many examples treated in the literature, we shall focus on two important systems, i.e. covalently linked and hydrogen-bonded ensembles: For example, when ZnTPP was covalently linked to a benzoquinone via a phenyl spacer in the *para* (*p*-P–*p*–Q) and *meta* (*m*-P–*p*–Q) positions, it was found that IET in *m*-P–*p*–Q is a much less favorable process than in *p*-P–*p*–Q [17]. Similarly, IET and the spectral changes in *cis* and *trans* isomers of a covalently linked porphyrin–cyclohexylene–quinone (PCQ) oriented in LCs were found to exhibit different line shape behavior and temperature dependence [15]. The different triplet RP transient spectra of the two isomers were interpreted in terms of their different molecular geometries. Moreover, in the case of the *trans* isomer, both triplet- and singlet-initiated ET routes could be detected concurrently (Fig. 1). These differences in the IET parameters are reflected by the free energy of the charge-separated states.

The influence of the particular spacer in tailor-made donor–acceptor systems may also be studied by the same approach. It should be mentioned that the nature of the spacer group is particularly important because of its influence on the electronic coupling between the donor and acceptor states. Thus different structures affect the magnitude of the spin–spin coupling (J) and the dipolar interaction (d), leading to different electron spin polarization (ESP) mechanisms, e.g. the RP mechanism (RPM) or the correlated radical pair mechanism (CRPM) [11, 18, 19]. Studies of ESP in RPs demonstrate how important it is to explore systematically the molecular structure (e.g. donor–acceptor distance and their mutual position) and its effect on the ESP pattern which allows one to identify the different IET processes. The requirement to identify a particular spin polarization mechanism called for utilization of high-field EPR spectroscopy, which, owing to its ultimate spectral and time resolution, revolutionized the detection ability of EPR systems [11, 20].

The chromophores of the *in vivo* photosynthetic reaction center are not covalently linked via a spacer group. Rather, they are held in space by the protein environment. An approach to model the primary ET events in photosynthesis involves the synthesis and study of preorganized supramolecular aggregates containing donors and acceptors which are not covalently linked. Along these lines, recent studies involved novel supramolecular structures in which molecular recognition was established via Watson–Crick base-pairing interaction [21] (Fig. 2). Specifically, a TREPR (X-band, 9.5 GHz) study was performed on H-bonded donor–acceptor complexes in which a guanine-functionalized zinc(II) porphyrin and a cytosine-functionalized dinitrobenzene were assembled in two types of LCs. In the nematic phase of the LCs, selective photoexcitation of the zinc(II) porphyrin moiety yields spin-polarized EPR signals, i.e. a broad absorptive/emissive spectrum and a superimposed narrow derivative-like signal. The rise of the narrow signal is accompanied by the decay of the broad signal, which is attributed to the lowest excited triplet state of the zinc(II) porphyrin. These findings are rationalized in terms of intra-ensemble ET (Fig. 1) occurring from the lowest excited triplet state of the donor (zinc(II) porphyrin) to the acceptor (dinitrobenzene) and by spin polarization effects [21, 22]. The narrow EPR signal is attributed to a long-distance charge-separated spin-correlated radical pair (SCRP). In the isotropic LC at higher temperatures a narrow absorptive EPR signal is observed regardless of the type of LC employed. This latter signal is assigned to a thermally populated SCRP.

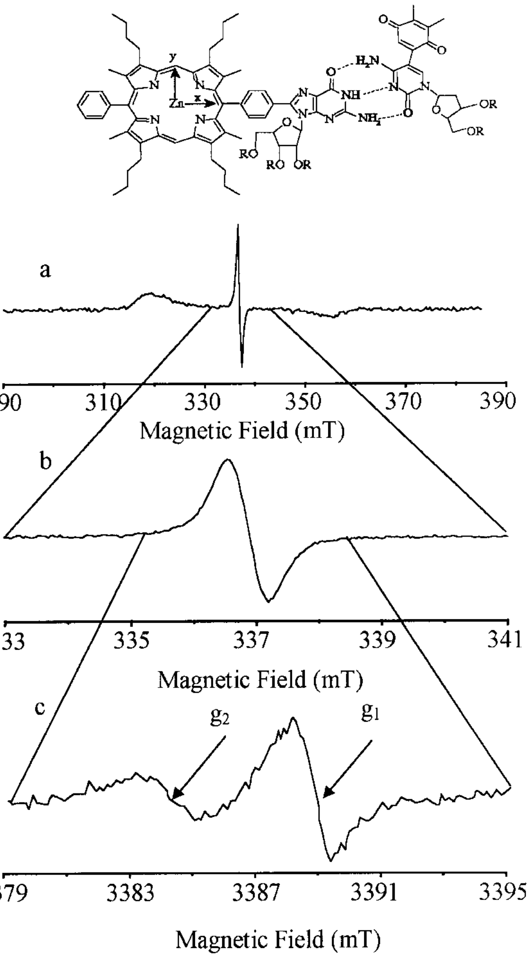

Fig. 2. Top: schematic structure of ZnG···QC, R ≡ SiMe$_2$Bu^t. The in-plane axes (x,y) of the porphyrin are shown on the molecular structure. (a) X-band TREPR spectra of [^{3}ZnP···DN] and the superimposed TRP ^{3}[ZnP$^{\cdot+}$···DN$^{\cdot-}$] (narrow signal) taken in the nematic phase of E-7 at 298 K, 450 ns after the laser pulse. (b) Expanded X-band TREPR spectrum of the TRP. (c) W-band TREPR spectrum of the TRP taken 250 ns after the laser pulse at 280 K in E-7. The measured g-values for the two species are 2.00275 and 2.00534 for ZnP$^{\cdot+}$ and DN$^{\cdot-}$ respectively (from Ref. [23]).

In order to identify the partners of the RP and thereby clarify the origin of the SCRP signal, W-band (94 GHz) high-field EPR experiments were performed [23]. These high Zeeman fields with a much better spectral resolution allow one to clearly differentiate between the two g-factors

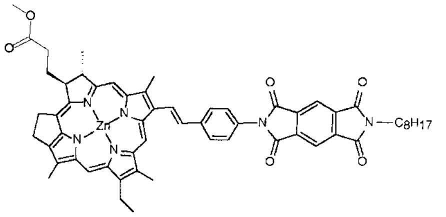

ZCPI

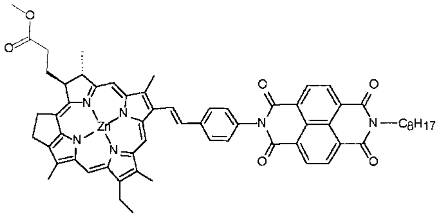

ZCNI

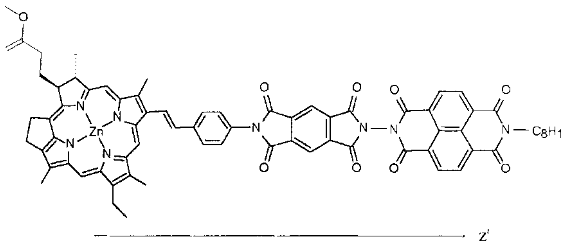

ZCPINI

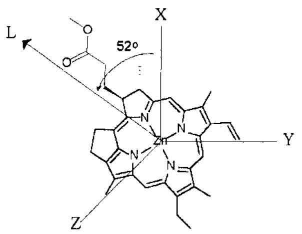

ZC

Fig. 3. Structures of the ZCPI, ZCNI and ZCPINI donor–acceptor systems (from Ref. [24]).

of both RP partners (Fig. 2). By comparison with known data, both the X- and W-band results show that a self-assembled complex is formed by nucleobase pairing and that intra-ensemble ET produces a weakly coupled SCRP of a porphyrin cation and a dinitrobenzene anion. In on-going TREPR studies at various microwave frequencies and Zeeman fields we are focusing on the details of base-paired interactions by specific H-bond networks as an effective tool for molecular recognition.

Determination of the Energy Levels of Radical Pair (RP) States in Photosynthetic Models

The driving force of the IET reaction depends strongly upon the location of the charge-separated energy states (Fig. 1). Thus it is important to develop experimental methods to explicitly determine the absolute values of the radical ion pair energy levels. This goal can be achieved by blending together molecular architecture, solvent properties (LCs) and fast TREPR detection of paramagnetic transients [24, 25]. This powerful approach has permitted the elucidation of photochemical mechanisms that otherwise could not be explored. The molecules under investigation in this study contain a chlorophyll-like electron donor (ZC) and two electron acceptors with different reduction potentials, A_1 (PI) and A_2 (NI). The compounds investigated were ZCPI, ZCNI and ZCPINI (Fig. 3) with donor–acceptor distances of $\sim$11, $\sim$11 and $\sim$18 Å respectively. These compounds have small but well-defined differences in their ion pair energies. They were dissolved in two LCs, E-7 and ZLI-1167 (Merck Ltd), with different dielectric constants and signs of the diamagnetic susceptibility $\Delta\chi$. The sign of $\Delta\chi$ determines the relationship between the director **L** and the external magnetic field **B**. A positive $\Delta\chi$ (E-7) results in the initial alignment of the dissolved molecules parallel to **B** ($\mathbf{L}\|\mathbf{B}$), while a negative $\Delta\chi$ (ZLI-1167) leads to perpendicular initial alignment ($\mathbf{L}\perp\mathbf{B}$). When oriented in LCs, these compounds undergo photoinduced IET to produce charge-separated states that can be monitored by TREPR. The energy level values and spin dynamics associated with the RP states depend strongly on the D–*s*–A structure, solvent reorganization energy and, most importantly, the temperature [16].

In Fig. 4 we show the time-evolved EPR spectra as a function of temperature. First, it should be mentioned that all three compounds exhibit a triplet spectrum at low temperature in the crystalline phase of the LC ($T < 250$ K). The RP signals are the narrow derivative-like signals superimposed on the wide triplet spectra. The spectra of $ZC^{\cdot+}PI^{\cdot-}$, contrary to $ZC^{\cdot+}NI^{\cdot-}$, clearly illustrate that $ZC^{\cdot+}PI^{\cdot-}$ has a lower driving force for charge separation as reflected by its spectrum, which is evident at relatively high temperature, whereas the $ZC^{\cdot+}NI^{\cdot-}$ spectrum is present at both temperatures. Furthermore, the spectra illustrate the large increase in the solvation ability of the soft glass, as an increase in temperature of only 10 K produces a strong signal from $ZC^{\cdot+}PI^{\cdot-}$. In addition to the temperature threshold for the appearance and disappearance of the RP spectra, important data are gained from the phase of the RP spectra. For a singlet-initiated RP the spectra of the triplet radical pairs (TRPs) $^3[ZC^{\cdot+}–PI^{\cdot-}]$ and $^3[ZC^{\cdot+}–NI^{\cdot-}]$ exhibit an absorption/emission (a/e) pattern. The opposite case, where the phase pattern is e/a, corresponds to a triplet-initiated RP. Inspection of Fig. 4 shows that at early times the singlet-initiated RPs dominate the spectrum, while later in time the triplet-initiated spectra take over. This phase inversion a/e → e/a occurs at a specific temperature and time, in full agreement with the value of the RP energies, and illustrates how powerful the TREPR method is when applied to IET processes.

In general terms, for a center-to-center distance $r < 12$ Å the TRP dominates the spectrum (the electron exchange interaction J is larger than the dipolar interaction d), while for $r > 12$ Å the dipolar interaction is dominant and leads to the correlated radical pair mechanism (CRPM) [24, 25]. The width of the RP spectrum can provide us with valuable information regarding the type of RP, i.e. whether it is a TRP or a CRP. It is evident that the RP spectra of ZCPI and ZCNI are due to TRPs and not CRPs. The latter mechanism is observed in D–*s*–A systems with center-to-center distance $r > 12$ Å. This conclusion is supported by comparing the spectra of $^3[ZC^{\cdot+}–PI^{\cdot-}]$ and $^3[ZC^{\cdot+}–NI^{\cdot-}]$ ($r \approx 11$ Å) with

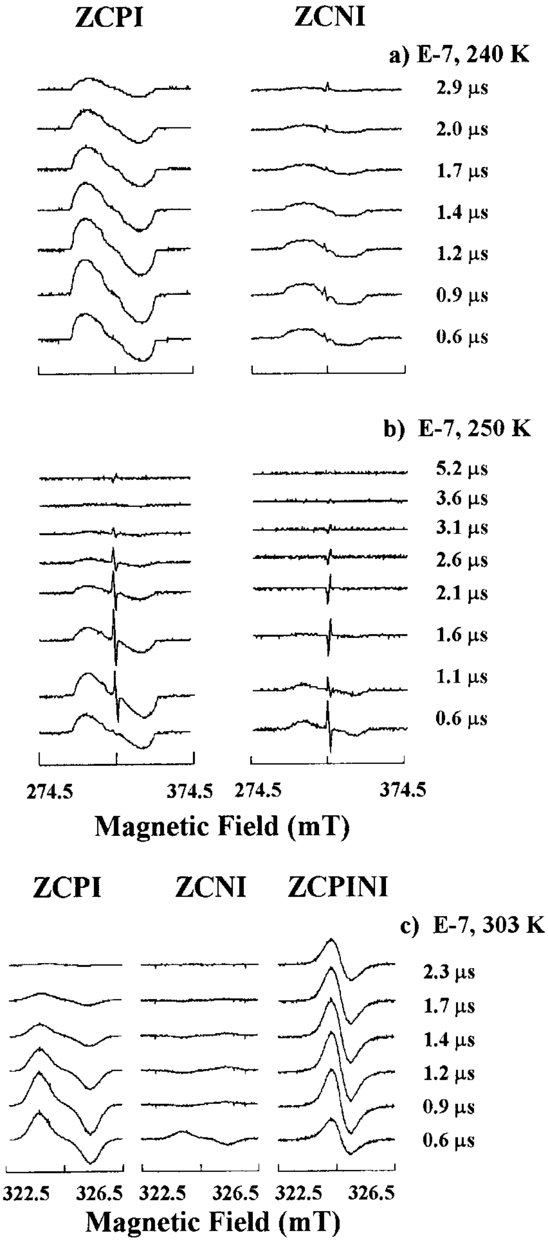

Fig. 4. TREPR spectra of photoexcited ZCPI, ZCNI (a–c) and ZCPINI (c) in E-7 at various temperatures and delay times after the laser pulse. Notice that the RP spectra of $ZC^{\cdot+}PINI^{\cdot-}$ correspond to triplet-initiated CRPs, while the spectra of $ZC^{\cdot+}PI^{\cdot-}$ and $ZC^{\cdot+}NI^{\cdot-}$ correspond to TRPs, which initially are singlet-initiated. The phase diagram of E-7 LC is crystalline $\xrightarrow{210K}$ soft glass $\xrightarrow{263K}$ nematic $\xrightarrow{333K}$ isotropic.

that of $ZC^{\cdot+}PINI^{\cdot-}$ ($r \approx 18$ Å), as shown in Figs 3 and 4c. For the pairs with short center-to-center distance a spectral width of ~1.6 mT corresponds, by using the point dipole approximation method of TRPs [24, 25], to a charge-separated distance of ~11.5 Å, which agrees well with the molecule dimension of 11 Å. In contrast to this, by assuming a TRP spectrum and with a spectral width of 0.65 mT for $ZC^{\cdot+}PINI^{\cdot-}$, a value of 15 Å is calculated for the pair separation. This value does not agree with the molecule dimension, which supports the conclusion that a CRP is generated in this case [24, 25].

RADICAL–PHOTOINDUCED TRIPLET INTERACTION

The Radical–Triplet Pair Mechanism

We start by providing the reader with a general background of the photophysical processes, which involves the interaction of stable radicals and triplets. These processes involves two mechanisms, i.e. the radical triplet pair mechanism (RTPM) and electron spin polarization transfer (ESPT). Both are related to the magnetic interaction between a stable paramagnetic radical and a photoexcited triplet molecule. This physical interaction results in basically the same radical and triplet, but the unpaired spin of the radical has an energy level population that now deviates substantially from thermal equilibrium. This process is linked to a broader phenomenon in spin chemistry called chemically induced dynamic spin polarization (CIDEP), first discovered in 1963 [26]. As mentioned above, the key parameter in CIDEP is the ESP phenomenon, which results in a non-Boltzmann spin population of the paramagnetic species involved in the various processes. Since the discovery of CIDEP, two main mechanisms have been associated with it, namely the triplet mechanism (TM) [27] and the radical pair mechanism (RPM) [28]. In the former the ESP is generated by selective intersystem crossing (ISC) from the photoexcited singlet to the triplet state, and in the latter the ESP is generated through collisions between radicals. Following the widespread use of lasers in EPR experiments, there have been some new observations of CIDEP of stable radicals in solution in the presence of photoexcited triplet chromophores. This polarization could not be explained by the above mechanisms and was treated theoretically [29–34] by the RTPM and ESPT, which are the main themes of this part of the paper.

So far, only the RTPM has received some rigorous theoretical treatment, which calculates the radical's polarization that is generated during its interaction with the photoexcited triplet. Current theories provide analytical [29, 35–37] and numerical [34] results for the dependence of the spin polarization upon the zero-field splitting (ZFS) parameter (D), solvent viscosity (η) and radical–triplet electron spin exchange (J). According to RTPM theory, the observed net polarization, which is equal for all hyperfine lines, depends on the precursor state (photoexcited singlet or triplet) and sign of J [38–41]. Thus for $J < 0$ the sign of polarization is negative for a triplet precursor and positive for a singlet one. The opposite holds for $J > 0$ [42]. Most of the early work on the RTPM was carried out on triplets with relatively high ZFS (small-sized molecules), for which the RTPM phenomenon is the strongest. This resulted in the need for UV excitation to generate the triplet and thus required the use of a flow system to avoid sample destruction during the experiment. More recently, additional work on the RTPM was performed with porphyrins, which can be excited by non-destructive visible light [33]. These experiments revealed the ESPT phenomenon, which is associated with magnetization transfer from the polarized triplet to the radical. This transfer resulted from the fact that the triplet, at the initial stages after light generation, is itself spin polarized owing to selected spin–orbit intersystem crossing. In relatively large molecules such as triplet porphyrins, with relatively small D but long spin–lattice relaxation time, this polarization survives long enough to be observed in the TREPR spectrum of the radical.

We can summarize the reactions involved in the interaction of a photoexcited triplet and a stable radical by extending the earlier [43] reaction scheme into:

$$\mathrm{P} \xrightarrow{h\nu} {}^{1*}\mathrm{P} \xrightarrow{\mathrm{ISC}} {}^{3*}\mathrm{P}_\mathrm{p} \qquad (1)$$

$$ {}^{3*}\mathrm{P} + \mathrm{R} \xrightarrow{\mathrm{RTPM}} \mathrm{R}_\mathrm{p} + \tfrac{2}{3}{}^{3*}\mathrm{P} + \tfrac{1}{3}\mathrm{P} \qquad (2)$$

$$ {}^{3*}\mathrm{P}_\mathrm{p} + \mathrm{R} \xrightarrow{\mathrm{ESPT}} \mathrm{R}_\mathrm{p} + {}^{3*}\,\mathrm{P}_\mathrm{p} \qquad (3)$$

$$ {}^{3*}\mathrm{P}_\mathrm{p} + {}^{3*}\,\mathrm{P}_\mathrm{p} \longrightarrow 2\mathrm{P} \qquad (4)$$

$$ {}^{3*}\mathrm{P}_\mathrm{p} \longrightarrow \mathrm{P} \qquad (5)$$

In these equations, P is the porphyrin which upon photoexcitation produces the photoexcited triplet $^{3*}\mathrm{P}_\mathrm{p}$ via ISC, and the subscript 'p' stands for a spin-polarized species. The processes described by equation (1) are usually very fast and are considered instantaneous on the TREPR timescale. Equation (2) describes the RTPM encounter where the triplet molecule interacts with the stable radical R. This interaction results in the radical and the triplet species, but with different polarization. Equation (3) describes an ESPT-type mechanism in which the radical encounters a polarized triplet. In this type of mechanism it is assumed that the radical does not quench the triplet and that the triplet polarization is transferred to the radical during the encounter. In contrast to this, the RTPM can only be 'activated' if the doublet levels, which represent one-third of the spin population during the encounter, have been depleted (Fig. 5b). This is accounted for by the fractional stoichiometrics in equation (2); namely, only one-third of the triplet population is in the doublet state during the encounter and is depleted to the ground state. It should be noted that every encounter between the radical and the triplet may lead to both ESPT and RTPM polarizations. Although both mechanisms operate simultaneously, one should note that the RTPM requires triplet quenching for polarization creation, while ESPT does not require triplet quenching [44].

Our initial work with porphyrin triplets interacting with stable radicals was aimed at better understanding and measuring the various types of polarization (ESPT and RTPM) which the radical gains. The majority of experimental techniques dealing with this problem were associated with using continuous-wave time-resolved EPR (CW-TREPR) spectroscopy [45] to monitor the transient radical spectrum after its interaction with the photoexcited triplet by the laser pulse. By careful analysis of the EPR kinetics, combined with independent knowledge of the rate constants involved, one can acquire a good estimate of the radical polarization. However, this method suffers some difficulties in obtaining the desired kinetic constants, which prevent extensive and accurate measurements of the radical polarization in systems under different external conditions, e.g. temperature. Moreover, the existence of two different time-dependent polarization processes (ESPT and RTPM) further complicates the problem to a degree, which cannot be overcome by CW-TREPR.

In light of these difficulties, a new approach has been introduced which uses the pulsed EPR (Fourier transform EPR (FT-EPR)) technique. By employing a pulse sequence which utilizes a special laser–microwave phase cycling (LMPC), one can circumvent the difficulties associated with the CW-TREPR method. As will be detailed below, the LMPC method enables one to elucidate the kinetic parameters associated with the set of equations (1)–(5). Thus, by analyzing our measurements, we found that substantial radical polarization could be generated in the RTPM process even without substantial quenching of the doublet levels, as will be detailed below.

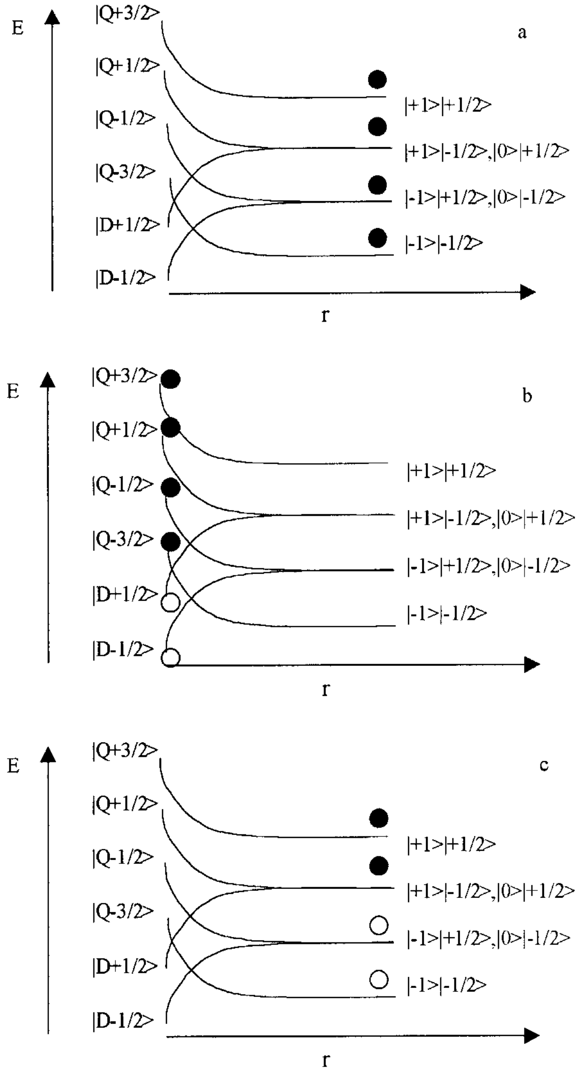

Fig. 5. A simple model for the polarization generated through a radical–triplet interaction. (a) When the distance between the triplet and the radical is large, the triplet Zeeman levels (1,0, −1) coincide with those of the radical ($+\frac{1}{2}, -\frac{1}{2}$). Upon approach, the angular momentum is added to form quartet (Q) and doublet (D) levels, which are split by the spin exchange interaction (*J*). The assumption is that in the initial stages of the encounter the levels are equally populated (full circles). (b) During the encounter, owing to spin conservation, the quartet levels cannot be depleted efficiently to the ground state. On the other hand, the doublet levels are quenched very efficiently and become empty. (c) Since the doublet levels are vacant, a substantial population is transferred from $\mathrm{Q}_{-3/2}$ and $\mathrm{Q}_{-1/2}$ to $\mathrm{D}_{\pm 1/2}$ in the crossing regions. Thus, after the separation, these levels are less populated and emissive spin polarization is generated.

Experimental Techniques and Results

First let us describe the method used to measure the radical polarization generated via the encounter with a photoexcited triplet. The LMPC method uses the following procedure. (a)

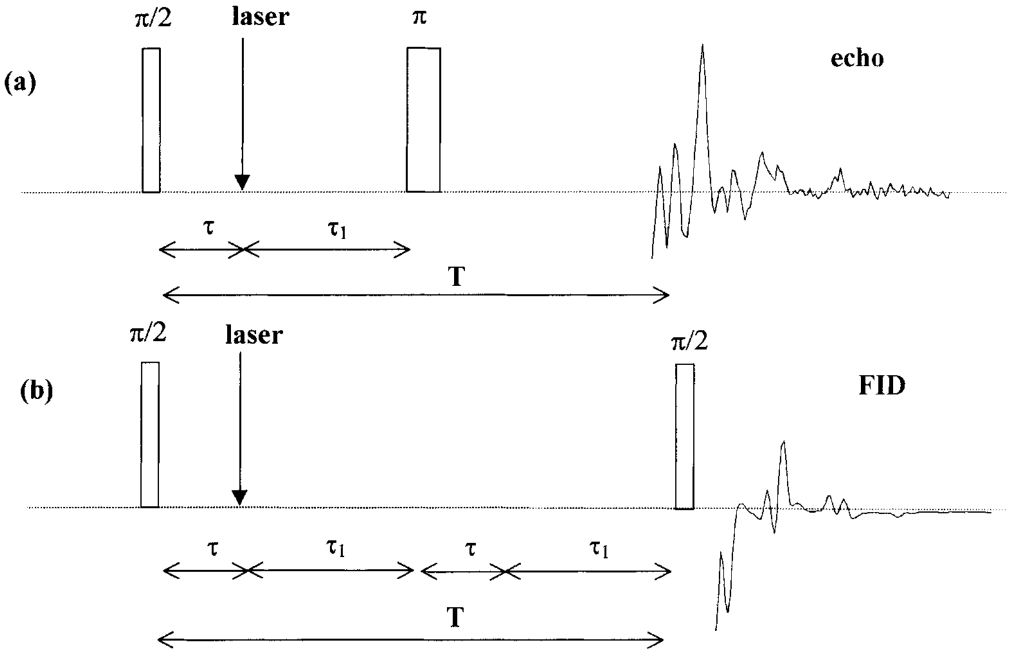

Fig. 6. (a) Echo pulse sequence to determine the rate of triplet–radical encounters. (b) FID pulse sequence to determine the *Z*-magnetization induced by the polarization processes. The duration of all the pulses is negligible. A typical echo and FID are also presented (from Ref. [43]).

In order to measure the rate of radical–triplet encounters, the pulse sequence $\pi/2$–τ–laser pulse–τ_1–π–echo detection is applied (Fig. 6a). The first pulse rotates the magnetization into the laboratory *XY*-plane, and without the laser pulse the sequence is a simple Hahn echo experiment. On the other hand, the laser pulse generates the triplets in solution (usually within a timescale of a few nanoseconds) which encounter the stable radicals. Each encounter results in a phase loss of the magnetization in the *XY*-plane while generating polarization along the *Z*-axis. Thus the encounters reduce the echo amplitude relative to the same microwave sequence, but with the laser pulse absent. (b) The second pulse experiment measures the magnetization along the *Z*-axis by the pulse sequence $\pi/2$–τ–laser pulse–$2\tau_1+\tau$–$\pi/2$–FID detection (Fig. 6b). This sequence is similar to the previous one, except for the fact that at the time of the echo appearance in the first sequence the *Z*-axis magnetization is now measured by FID. A detailed mathematical analysis of these pulse sequences

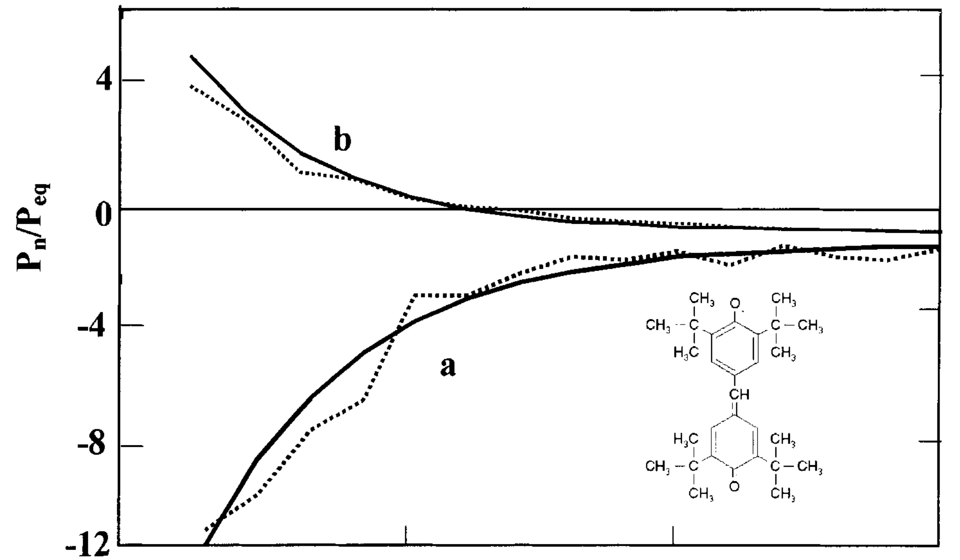

Fig. 7. (a) Polarization curve of Gal–H_2TPP as a function of time after the laser pulse (dotted line), fitted by the theoretical curve (full line). The abscissa represents the time after the laser pulse (see Fig. 6). The lines represent a gradual transition from radical polarization which is dominated by ESPT to that dominated by the RTPM. This transition is made with exponential time dependence, which corresponds to the triplet spin–lattice relaxation time. (b) The same as (a), but for a Gal–ZnTPP system (from Ref. [43]).

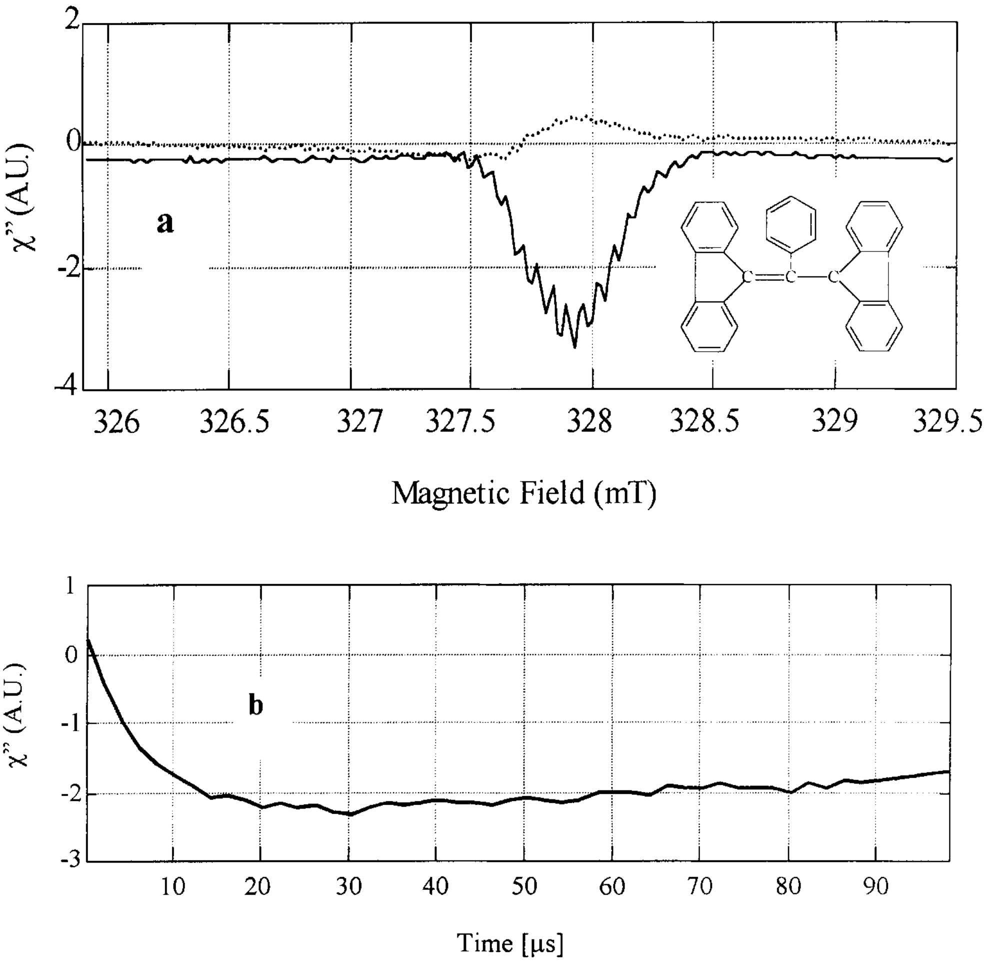

Fig. 8. (a) FT-EPR spectra of BDPA with H_2TPP before laser light excitation (dotted line) and 50 μs after laser excitation (full line). (b) Magnetization measurement of the H_2TPP–BDPA system. The thermal magnetization is measured at the first point of the kinetics curve before laser excitation at 0.5 μs. Photoexcitation creates the magnetization with a negative sign in strong emission (~10 times larger than the thermal magnetization). The long-lived polarized magnetization corresponds to inefficient quenching of the triplet by the radical. This keeps the triplet population almost constant on a timescale of submilliseconds.

shows how the radical polarization at various times after the laser pulse can be measured [43].

The radical polarization versus time as measured by this method is presented in Fig. 7. It can be seen that in the initial stage after laser excitation the triplet is still polarized and contributes considerably to the polarization of the radical. However, after the triplet relaxes to a Boltzmann spin population (within the triplet spin lattice relaxation time T_1), the RTPM process is dominant. One should also note that these measurements enable an accurate determination of the triplet T_1 in solution without actually measuring its EPR spectrum.

Another important aspect of the radical–triplet interaction is related to the triplet state after its encounter with the radical. Previous studies of the RTPM assumed that the doublet level population of the triplet–radical pair is depleted completely to the ground state during the encounter (Fig. 5b). This implies a substantial depletion of the triplet population as well. To examine this assumption more quantitatively, we have recently carried out some experiments with porphyrins and BDPA (Fig. 8) in a mixture of 20% dichloromethane and 80% paraffin oil of high viscosity. Such a viscosity made it possible to observe the kinetics of the magnetization development more easily on a timescale of submilliseconds. Under these conditions the triplet–triplet quenching is negligible, and without introducing the free radical to the solution, the triplet porphyrin can live for up to several milliseconds (in a concentration of several mM). By dissolving the stable radical in the solution, the lifetime of the triplet decreases, because an additional quencher is introduced into the system. However, as a result of our recent experiments we have found solid evidence that the triplet quenching does not follow the stoichometrics of equation (2). In other words, not one-third of the triplet population is quenched in each radical–triplet encounter of the RTPM type [44]. These findings are shown in Fig. 8. It can be seen that after the initial development of the magnetization in the emission mode, quasi-equilibrium is approached. This implies that polarized radicals are constantly generated without a considerable quenching of the triplet. Careful analysis of these results [44] shows that that this type of kinetics corresponds to about 1/30 of triplet quenching in every encounter with the radical, and not one-third as inferred from equation (2).

CONCLUSIONS

It has been shown how porphyrins and porphyrin derivatives participate in two interesting photophysical processes in which the electron spin plays an important role. In IET studies the unique properties of the porphyrins as electron donors allow one to obtain information regarding the genesis of the electron transfer route and identify unambiguously the products of the IET reactions. Furthermore, the investigation of D–*s*–A systems using a porphyrin as a donor provides quantitative information concerning the ordering of the radical ion pair energy levels relative to the known excited state energy levels of the porphyrin moiety.

In doublet–triplet interactions the photoexcited porphyrin can generate polarization in the stable radical via two routes. The first one corresponds to the polarization of the porphyrin itself and is apparent during the spin–lattice relaxation time of the porphyrin. The second one corresponds to the polarization generated in the radical, regardless of the porphyrin polarization, and extends beyond the spin–lattice relaxation time of the porphyrin. The differentiation between these two mechanisms enables an accurate determination of the porphyrin spin–lattice relaxation time without direct measurement of its EPR spectrum (which is seldom possible in liquid solutions). An additional interesting feature of the radical–triplet interaction, which was observed in our experiments, is the relatively small depletion of the triplet porphyrin to the singlet state during the RTPM encounter.

Acknowledgements

This work was partially supported by a US–Israel BSF grant, by the Volkswagen Foundation (I/73 145) and by the Israel Ministry of Science. The Farkas Research Center is supported by the Bundesministerium für die Forschung und Technologie and the Minerva Gesellschaft für Forschung GmbH, Germany.

REFERENCES

1. Möbius K. *Isr. J. Chem.* 1988; **28**: 57.
2. Debreczeny MP, Svec WA, Wasielewski MR. *Science* 1996; **274**: 584.
3. Wiederrecht GP, Yoon BA, Wasielewski MR. *Science* 1995; **270**: 1794.
4. Blank A, Kastner R, Levanon H. *IEEE Trans. Microwave Theory Techniq.* 1998; **46**: 2137.
5. Wiederrecht GP, Niemczyk MP, Svec WA, Wasielewski MR. *J. Am. Chem. Soc.* 1996; **118**: 81.
6. Von Gersdorff J, Huber M, Schubert H, Niethammer D, Kirste B, Plato M, Möbius K, Kurreck H, Eichberger R, Kietzmann R, Willig F. *Angew. Chem. Int. Ed. Engl.* 1990; **29**: 670.
7. Sessler JL, Wang B, Harriman A. *J. Am. Chem. Soc.* 1993; **115**: 10418.
8. Sessler JL, Wang B, Harriman A. *J. Am. Chem. Soc.* 1995; **117**: 704.
9. Gonen O, Levanon H. *J. Phys. Chem. A.* 1985; **89**: 1637.
10. Levanon H. *Rev. Chem. Intermed.* 1987; **8**: 287.
11. For a recent review on EPR in biological systems, see e.g. Levanon H, Möbius K. *Annu. Rev. Biophys. Biomol. Struct.* 1997; **26**: 495.
12. Sumida JP, Liddell PA, Lin S, Macpherson AN, Seely GR, Moore AL, Moore TA, Gust D. *J. Phys. Chem.* 1998; **102**: 5512.
13. Elger G, Wiehe A, Möbius K, Kurreck H. *Z. Phys. Chem.* 1999; **213**: 181.
14. Regev A, Levanon H, Murai T, Sessler JL. *J. Chem. Phys.* 1990; **92**: 4718.
15. Hasharoni K, Levanon H, von Gersdorff J, Kurreck H, Möbius K. *J. Chem. Phys.* 1993; **98**: 2916.
16. Levanon H, Hasharoni K. *Prog. React. Kinet.* 1995; **20**: 309.
17. Hasharoni K, Levanon H, Gätschmann J, Schubert H, Kurreck H, Möbius K. *J. Phys. Chem. A.* 1995; **99**: 7514.
18. Morris AL, Norris JR, Thurnauer MC. In *Reaction Centers of Photosynthetic Bacteria*. Michel-Beyerle ME (ed.). Springer-Verlag: Berlin, 1990; 423.
19. Closs GL, Forbes MDE, Norris JR. *J. Phys. Chem. A.* 1987; **91**: 3592.
20. Budil DE, Earle KA, Lynch WB, Freed JH. In *Advanced EPR. Application in Biology and Biochemistry*. Hoff AJ (ed.). Elsevier: Amsterdam, 1989; 307.
21. Asano-Someda M, Levanon H, Sessler JL, Wang R. *Mol. Phys.* 1998; **95**: 935.
22. Berman A, Izraeli ES, Levanon H, Wang B, Sessler JL. *J. Am. Chem. Soc.* 1995; **117**: 8252.
23. Berg A, Shuali Z, Asano-Someda M, Levanon H, Fuhs M, Möbius K, Wang R, Sessler JL. *J. Am. Chem. Soc.* 1999; **121**: 7433.
24. Levanon H, Galili T, Regev A, Wiederrecht GP, Svec W, Wasielewski MR. *J. Am. Chem. Soc.* 1998; **120**: 6366.
25. Wiederrecht GP, Svec W, Wasielewski MR, Galili T, Levanon H. *J. Am. Chem. Soc.* 1999; **121**: 7726.
26. Fessenden RW, Schuler RH. *J. Chem. Phys.* 1963; **39**: 2147.
27. Wong SK, Wan JSK. *J. Am. Chem. Soc.* 1972; **94**: 7197.
28. Adrian FJ. *Rev. Chem. Intermed.* 1979; **3**: 3.
29. Goudsmit G-H, Paul H, Shushin AI. *J. Phys. Chem. A.* 1993; **97**: 13243.
30. Kawai A, Obi K. *Rev. Chem. Intermed.* 1993; **19**: 865.
31. Rozenshtein V, Zilber G, Rabinovitz M, Levanon H. *J. Am. Chem. Soc.* 1993; **115**: 5193.
32. Turro NJ, Koptyung IV, Van Willigen H, McLauchlan KA. *J. Magn. Reson.* 1994; **109**: 121.
33. Fujisawa JI, Ohba Y, Yamauchi S. *J. Phys. Chem. A.* 1997; **101**: 434.
34. Kobori Y, Takeda K, Tsuji K, Kawai A, Obi K. *J. Phys. Chem. A* 1998; **102**: 5160.
35. Shushin AI. *J. Chem. Phys.* 1993; **99**: 8723.
36. Shushin AI. *Chem. Phys. Lett.* 1993; **208**: 173.
37. Dutt GB, Periasamy NJ. *J. Chem. Soc., Faraday Trans.* 1991; **87**: 3815.
38. Imamura T, Onitsuka O, Obi K. *J. Phys. Chem. A* 1986; **90**: 6744.
39. Friedenberg A, Levanon H. *Chem. Phys. Lett.* 1976; **41**: 84.
40. Lok MT, Tehan FJ, Dye JL. *J. Phys. Chem. A* 1972; **76**: 2975.
41. Kawai A, Obi K. *J. Phys. Chem. A* 1992; **96**: 52.
42. The polarization is defined as $P = (n_\beta - n_\alpha)/(n_\beta + n_\alpha)$, where n_α and n_β are the populations in the upper and lower magnetic levels respectively.
43. Blank A, Levanon H. *J. Phys. Chem. A.* 2000; **104**: 794.
44. Blank A, Levanon H. Submitted for publication.
45. For a review article, see e.g. McLauchlan KA. In *Advanced EPR. Application in Biology and Biochemistry*. Hoff AJ (ed.). Elsevier: Amsterdam, 1989; 345.